

THE MOTION OF A LOSING MASS PLASMON

P.R. RIVERA-ORTIZ^{1,2}, A. RODRÍGUEZ-GONZÁLEZ^{1,2}, L. HERNÁNDEZ-MARTÍNEZ¹ & J. CANTÓ³

Accepted version February 7, 2019

ABSTRACT

The interaction of a high velocity clump of gas has been described by the plasmon model, which considers balance between ram pressure and the internal stratified structure of the decelerated clump. In this paper we propose an analytical model to describe the mass loss of such a clump due the interaction with the environment, describing its influence on the plasmon dynamics. We carry out comparisons between an analytic model and axisymmetric gasdynamic simulations of plasmon evolution. From our simulations we were able to find the values of the friction constants α and λ . Comparing with the complete analytic model from which we can infer the position and the mass loss of the clump as function of the clump's density and the environment ratio.

Subject headings: ISM: general – ISM: kinematics and dynamics – ISM: jets and outflows – shock waves

1. INTRODUCTION

The problem of a wind/molecular cloud interaction has been long studied in the past. De Young & Axford (1967, hereafter DA) described the motion of a clump decelerated by the ram pressure and determined the lifetime of the plasmon. They applied this model to Cygnus A and concluded that analyzing the dynamics of plasmons should reduce their free parameters. It became a very popular model to explain confinement of radio lobes propagating through the intergalactic medium (Ubachukwu, Okoye & Onuora 1991; Daly, 1994), models of radio-loud quasars (Daly, 1995) and models of the optical narrow-line regions of Seyfert galaxies (Taylor, Dyson & Axon 1992; Veilleux, Brent & Bland-Hawthorn, 1993). Cantó et al., (1998; hereafter C98) rederived the plasmon solution adding the centrifugal pressure to obtain a modified plasmon profile.

In most cases it is difficult to calculate the real age of an astronomical plasmon since there is no clear information about deceleration and most of plasmons are isolated so there is not enough information about the static medium. To solve this problem a set of several plasmons with an noticeable deceleration moving under similar restrictions is needed.

Orion BN/KL is an ideal laboratory to prove the plasmon solution, because has an almost isotropic and explosive outflow that could be produced by the non-hierarchical close dynamic interaction of a forming multiple-star system (Zapata, 2009). In this region there are more than a hundred of filamentary structures known as fingers that allow to estimate a dynamical age between 1000 years and 500 years, assuming no deceleration. Nevertheless, there is observational evidence that the longest fingers detected in H₂ emission are losing speed, probing their interaction with the environment (Bally et al. 2011). It is a very interesting star formation region that due to

its distance, at 414 pc, allows us to determine its characteristics with enough detail. Therefore, we also can model the physics using theoretical and numerical models, using some observational constrains. Some of these models have achieved important results as determining the dynamical age and the energy of the explosive event. Nevertheless there are important questions that deserve attention and are not resolved yet, such as the real age of the event, the mechanism that can generate such distribution of the fingers, as well as their ejection velocity since there is evidence of a drag force.

The effect of a drag force is necessary to understand the real motion of a plasmon. Several numerical simulations have shown a deceleration effect greater than the expected by ram pressure (Yalinewich & Sari, 2016), but it has not been deeply analyzed since cooling effects were not included.

The destruction of the original clump was also considered in Raga et al. (1998) in their study of the interaction of a fast wind impinging a compact spherical cloud. They concluded that the motion is affected by the detachment of material of the cloud, which results in a limited application of their model.

Then, the assumption that a clump has no deceleration or a deceleration according to models with constant mass, can lead to overestimate the age of astrophysical outflows.

In this work, we use the DA solution to propose a mass loss rate for a plasmon and we obtained its equation of motion. We compare results of this analytic model with numerical simulations using Orion BN/KL plausible ejection conditions. We presented an analytic (§ 2) and numerical (§ 3) models of a deceleration of the clumps as function of ratio density when the mass loss rate is considered. We present a comparison between the analytic and numerical models and a prediction of the lifetime of clumps assuming similar conditions to the system Orion BN/KL is presented in § 4. Finally, we present our conclusions in § 5.

2. ANALYTICAL MODEL

2.1. *De Young & Axford's plasmon*

Electronic address: pedro.rivera@correo.nucleares.unam.mx
¹Instituto de Ciencias Nucleares, Universidad Nacional Autónoma de México, Ap. 70-543, 04510 D.F., México
²LUTH, Observatoire de Paris, PSL, CNRS, UMPC, Univ Paris Diderot, 5 place Jules Janssen, F-92195 Meudon, France
³Instituto de Astronomía, Universidad Nacional Autónoma de México, Ap. 70-264, 04510 D.F., México

DA studied the problem of a clump of gas moving through an uniform environment. They found a solution (the 'plasmon' solution) based on the balance between the ram pressure of the environment and the stratified thermal pressure of the decelerating clump. For a clump of mass M , isothermal sound speed c , moving supersonically with velocity v through a medium of density ρ_a , the plasmon adopts a pressure and density stratification given by

$$P = P_0 e^{-x/h}, \quad \rho = \rho_0 e^{-x/h}, \quad (1)$$

as a function of the position x from the tip of the cloud where the pressure is P_0 , the density is $\rho_0 = P_0/c^2$, where c is the isothermal speed of sound. Ram pressure with the environment with density ρ_a indicates $P_0 = \rho_a v^2$.

In Eq. (1)

$$h = \frac{c^2}{a}, \quad (2)$$

is the scaleheight of the pressure distribution, and a the deceleration of the clump.

The balance between the internal pressure and the ram pressure with the surrounding environment shapes the plasmon as,

$$y = 2h \arctan(e^{x/h} - 1)^{1/2}. \quad (3)$$

Then, the mass of the moving clump of gas is related to the shape by the material enclosed by y ,

$$M = \int_0^\infty \pi \rho y^2 dx = \xi_{DA} \frac{\rho_a v^2 h^3}{c^2}, \quad (4)$$

where $\xi_{DA} = \frac{\pi}{2}(\pi^2 - 4)$.

2.2. Mass loss rate

We propose a mass loss rate per unit area, μ , which depends on the density and the internal sound speed, c ,

$$\mu = \lambda \rho c, \quad (5)$$

where λ is an unknown parameter expected to be less than one. Behind Eq. (5), there is the assumption that the clump loses mass at a rate per unit area proportional to the local mass density, ρ , and with a subsonic velocity λc . This hypothesis have been proposed and tested, for instance, by Kahn (1980), Cantó and Raga (1991) and Raga, Cabrit and Cantó (1995) in their studies of the turbulent mixing layers produced by the interaction of interstellar outflows. An estimation of λ , in our case, is found by comparison with our numerical simulation of the problem.

Therefore, the total mass loss rate is given by the integration of μ over the total surface of the plasmon,

$$\dot{M} = \int_0^\infty \mu dA = \lambda \xi_{DA} \left(\frac{8}{\pi + 2} \right) \frac{\rho_a v_0^2 h^2}{c}, \quad (6)$$

Dividing Eq. (4) by Eq. 6 and using Eq. (2) we obtain the differential equation,

$$\frac{1}{M} \frac{dM}{dv} = \frac{8\lambda}{(\pi + 2)c}. \quad (7)$$

We can use a dimensionless version of Eq. (7) with the following definitions,

$$m = M/M_0, \quad u = v/v_0, \quad \alpha = \frac{8\lambda v_0}{(\pi + 2)c}, \quad (8)$$

where M_0 is the initial mass and v_0 is the initial velocity of the plasmon. The solution to Eq. (7) is

$$m = e^{\alpha(u-1)}, \quad (9)$$

which relates that mass behavior as function of the plasmon speed with the constant α .

The equation of motion of the plasmon is,

$$\frac{dv}{dt} = -a. \quad (10)$$

Solving Eq. (4) for h , Eq. (2) for a , and substituting in Eq. (10), we find the equation of motion in a non-dimensional form

$$\frac{du}{d\tau} = - \left(\frac{u^2}{m} \right)^{1/3}, \quad (11)$$

where

$$\tau = t/t_0, \quad t_0 = \left(\frac{M_0 v_0}{\xi_{DA} \rho_a c^4} \right)^{1/3}. \quad (12)$$

Eq. (11), together with Eq. (9), has the formal solution,

$$\tau = \int_u^1 u^{-2/3} e^{-\frac{\alpha}{3}(1-u)} du. \quad (13)$$

The position of the clump after ejection R is found by solving the kinematic equation,

$$\frac{dR}{dt} = v \quad (14)$$

Defining $r = R/(v_0 t_0)$ and combining it with Eq. (14), we find the solution

$$r = \int_u^1 u^{1/3} e^{-\frac{\alpha}{3}(1-u)} du. \quad (15)$$

Then Eq. (9), Eq. (13), and Eq. (15) give the mass m , velocity u and position r of the clump after a time τ of ejection, using u as the free variable in the interval $[0,1]$.

The clump halts at a finite time τ_f and finite distance r_f with finite mass m_f . These limits are determined by the condition $u = 0$ in Eq. (9), Eq. (13) and Eq. (15) and are functions of α only. We can find useful approximations in the limits $\alpha \ll 1$:

$$\tau_f \simeq 3 \left(1 - \frac{\alpha}{4} \right), \quad (16)$$

$$r_f \simeq \frac{3}{4} \left(1 - \frac{\alpha}{7} \right), \quad (17)$$

which are consistent with the DA solution. Furthermore, for $\alpha = 0$ in Eq. (13) and Eq. (15) we recover the solution of DA.

Also, there are some interesting results concerning the stopping time τ_f and distance r_f that deserve to be highlighted.

First, we must notice that independent of the physical characteristics of the original clump (shape, density structure or internal sound speed), the initial interaction

with the medium through which it moves will modify these characteristics to those of a plasmon. That is, its shape will be transformed to that given by Eq. (3), its pressure and density stratification given by Eq. (1) and so on. This transformation is actually accomplished by a reverse shock that moves inside the original clump, changing it into a plasmon.

As we have seen above the structure of the plasmon is highly dependent on its internal sound speed i.e., on its temperature). Let us assume that the temperature of the newly formed plasmon is the one left by the reverse shock that moved through it. For simplicity, let also assume that this shock is planar and strong. In the Appendix we show that the corresponding isothermal sound speed is,

$$c = v_0 \left(\frac{\gamma - 1}{2} \right)^{1/2} \beta, \quad (18)$$

where $\beta = \sqrt{\rho_a/\rho_{cl}}$ is the square root of the ratio of the density of the environment and the density of the original clump. Using Eq. (18) in Eq. (8) we find

$$\alpha = \frac{8\lambda}{\pi + 2} \sqrt{\frac{2}{\gamma - 1}} \left(\frac{1}{\beta} \right), \quad (19)$$

which is independent of the velocity v_0 and depends only on the ratio β . Next, let us consider the time t_f for the clump to stop. It is given by

$$t_f = t_0 \tau_f(\alpha), \quad (20)$$

where t_0 is defined by Eq. (12) as,

$$t_0 = \left(\frac{M_0 v_0}{\xi_{DA} \rho_a c^4} \right)^{1/3}, \quad (21)$$

or

$$t_0 = \left[\frac{M_0}{\xi_{DA} \rho_a} \left(\frac{v_0}{c} \right)^4 \right]^{1/3} \frac{1}{v_0}, \quad (22)$$

and corresponds to the timescale used by DA in their solution to estimate the lifetime of a plasmon (Eq. (27)).

As shown in the Appendix (see also Eq. (20)) the ratio v_0/c is only function of the contrast density β and independent of the velocity v_0 . Thus, given the ratio β , the time t_0 and therefore the time t_f for the clump to stop diminish as the initial velocity of the clump increases. This is an unexpected result: the time for stopping a stripping clump is inverse with its initial velocity. Faster clumps stop earlier independent of their size. Now, let us consider the stopping distance R_f . This is given by,

$$R_f = v_0 t_0 r_f(\alpha), \quad (23)$$

From the discussion above, the product $v_0 t_0$ results independent of v_0 , and thus R_f . Then, clumps with the same ratio β stop at the same distance from the injection point, independent of either its initial velocity or size.

3. AXISYMMETRIC SIMULATIONS OF PLASMON EVOLUTION

3.1. The numerical setup

In order to validate the analytical model, we have computed axisymmetric numerical simulations with the full radiative gasdynamic equations. We used the WALKIMYA 2D code (see Castellanos-Ramírez et al.

2018 and Esquivel et al. (2010)) to perform all numerical simulations. The code solves the hydrodynamic equations and chemical networks on a two dimensional Cartesian adaptive mesh, using a second order finite volume method with HLLC fluxes (Toro et al. 1994).

The adaptative mesh consist of four root blocks of 16×16 cells, with 7 levels of refinement, yielding a maximum resolution of 4096×1024 (axial \times radial) cells. The boundary conditions used on the symmetry axis are reflective and the other ones are outflows. The size of the mesh is large enough so that the choice of outer boundaries does not affect the simulation.

The energy equation includes the cooling function described by Raga & Reipurth (2004) for atomic gas and for lower temperatures we have included the parametric molecular cooling function presented in Kosiński & Hanasz, 2007,

$$\Lambda_{\text{mol}}(T) = L_1 \cdot T^{\epsilon_1} + L_2 \cdot \exp\left(-\frac{c_*}{(T - T_*)^{\epsilon_2}}\right), \quad (24)$$

for $T < 5280$ K, where, $\epsilon_1 = 10.73$, $\epsilon_2 = 0.1$, $L_1 = 4.4 \times 10^{-67}$ erg cm³ s⁻¹ K^{- ϵ_1} , $L_2 = 4.89 \times 10^{-25}$ erg cm³ s⁻¹, $c_* = 3.18$ K ^{ϵ_2} and $T_* = 1$. K. The total radiative energy for temperatures lower than 5280 K is given by,

$$L_{\text{rad},\text{mol}} = n_{\text{gas}} \cdot n_{\text{CO}} * \Lambda_{\text{mol}}(T) \quad (25)$$

where, n_{gas} and n_{CO} is the numerical density of the gas and the CO molecule, respectively.

We have also considered the heating of the gas via cosmic rays, using the heating rate presented in Henney et al. (2009),

$$\Gamma_{\text{crp}} = 5 \times 10^{-28} n_{\text{H}} \text{ erg s}^{-1} \quad (26)$$

where, n_{H} is the numerical density of the all the hydrogen species.

3.2. Numerical models of the plasmon evolution

In order to study the deceleration of a high velocity clump we use compatible parameters with the ejection of Orion Fingers in Orion BN/KL. We have run numerical simulation assuming that the computational domain was initially filled by a homogeneous, stationary ambient medium with temperature $T_{\text{env}} = 100$ K and various densities (see below). The numerical integration had a domain with physical size of 48000×12000 AU on each side, with a maximum resolution (along the two axes) of 11.7 AU. We carried out time integration from $t_i=0$ to $t_f=1000$ yr, and the clump is released at $z=700$ AU for all models. An estimation of the initial mass in each of the clumps is $m_{\text{cl}} = 0.03 M_{\odot}$ since the total mass of the moving gas in the ~ 400 fingers in Orion BN/KL is about $8 M_{\odot}$ (Bally, 2016). Also, the observed transverse size of the fingers is about 400 AU.

In the numerical models, the initial clump is imposed as a sphere of radius $R_{\text{cl}}=50$ AU, corresponding to 4 pixels at the maximum resolution of the adaptive grid and with an uniform density of $n_{\text{cl}}=1 \times 10^{10}$ cm⁻³. Since the initial clump is out of equilibrium, it increases its size to about 400 AU from the first output, and then the density structure of a plasmon arises.

We have computed ten simulations of the clumps, varying the density of the interstellar medium and the velocity at which the clump was thrown (see Table 1).

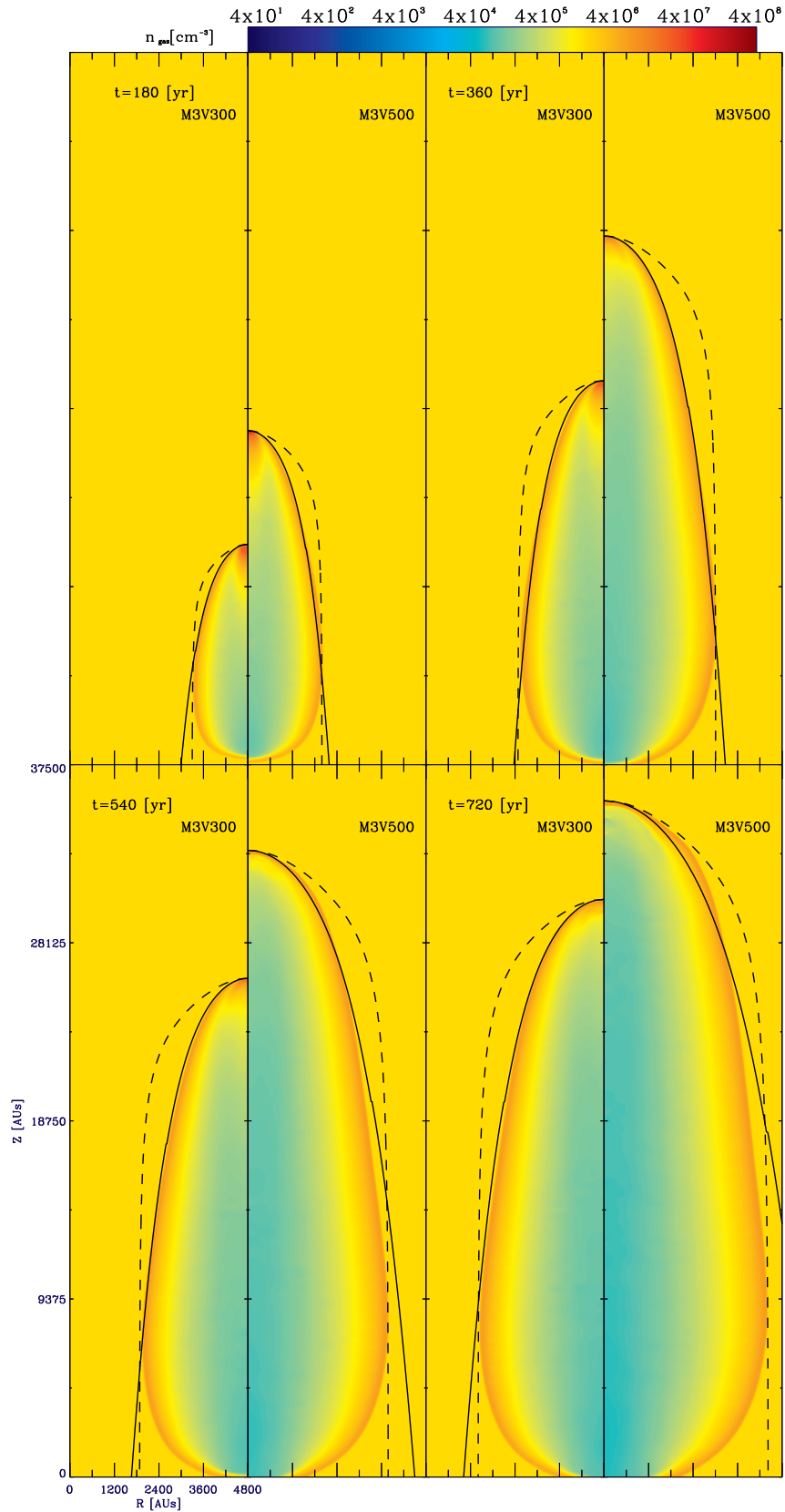


FIG. 1.— Snapshots from the numerical simulations showing the numerical density. Each panel compares two models with initial velocity of 300 (left) and 500 (right) km s^{-1} at $t = 180, 360, 540$ and 720 years. Lines are the analytical fit, dashed lines of DA, solid lines our fit

TABLE 1
INITIAL CONDITIONS OF THE NUMERICAL MODELS

Models	Environment	clump
	n_a [cm^{-3}]	v_0 [km s^{-1}]
M1V300/M1V500	1.0×10^6	300/500
M2V300/M2V500	3.16×10^6	300/500
M3V300/M3V500	1.0×10^7	300/500
M4V300/M4V500	3.16×10^7	300/500
M5V300/M5V500	1.0×10^8	300/500

One of the main hypothesis of our analytic model is that the early interaction of the original clump with the environment will modify its initial characteristics (shape, density stratification or sound speed) to those of a plasmon. The sound speed of the moving clump is calculated using the internal temperature, which is about 15 K and is in the order of magnitude of the sound speed obtained with Equation A14

In order to illustrate the numerical simulation results, in Figure (1) we present the density maps for models M3V300 and M3V500 (left and right panels, respectively) at evolutionary time of 180, 360, 540 and 720 yr, top left, top right, bottom-left and bottom right panels, respectively. The solid lines, in all the panels, are the analytical fit of the plasmon shape, Eq. (16) and Eq. (17) presented in C98 and the dashed lines are also the plasmon shape's fit obtained by DA in their Eq. (2). In both models, the plasmon shape expected by the DA equation is wider than the shape of the plasmon's head obtained in the numerical simulations. For model M3V500 (the right panels of Figure (1)) the plasmon shape proposed by C98 is in very good agreement with the numerical simulations, at least up to $t \sim 500$ yr. After this time, the plasmon (of the model M5V300) is rapidly decelerated and the bow shock changes in a different shape that the one proposed by C98. The models with lower initial velocity, model M3V300, does not have an appreciable deceleration and the numerical simulation shape is in agreement with the C98 prediction.

Other prediction of our model is that the dimensionless mass m of the clump is related to its dimensionless velocity u by Eq. (9). We can test this prediction. The top panel of Figure 2 shows the position as function of time by plasmon for the models with initial velocity of 300 km s^{-1} (see Table (1)). The squares, asterisk, triangles, plus and diamond symbols are drawing the results obtained for the models evolving with logarithmic interstellar medium densities of 6, 6.5, 7, 7.5 and 8, respectively. As we can see, the position is smaller for models that evolve in denser environments, it means the deceleration or decrease on the plasmon's velocity, as function of time (see middle panel of Figure (2)) is larger in models with larger ram pressure (Eq. (A6)). And in the bottom panel of this figure, we presented the mass of the clump as function of time. We calculated the mass considered the gas into the sphere of 50 AU of radii since the clump position and we also note that the denser interstellar medium produce a larger mass loss rate in the clumps moving in environments with uniform density and temperatures. In the same way, Figure (3) shows the position, velocity and mass as function of time

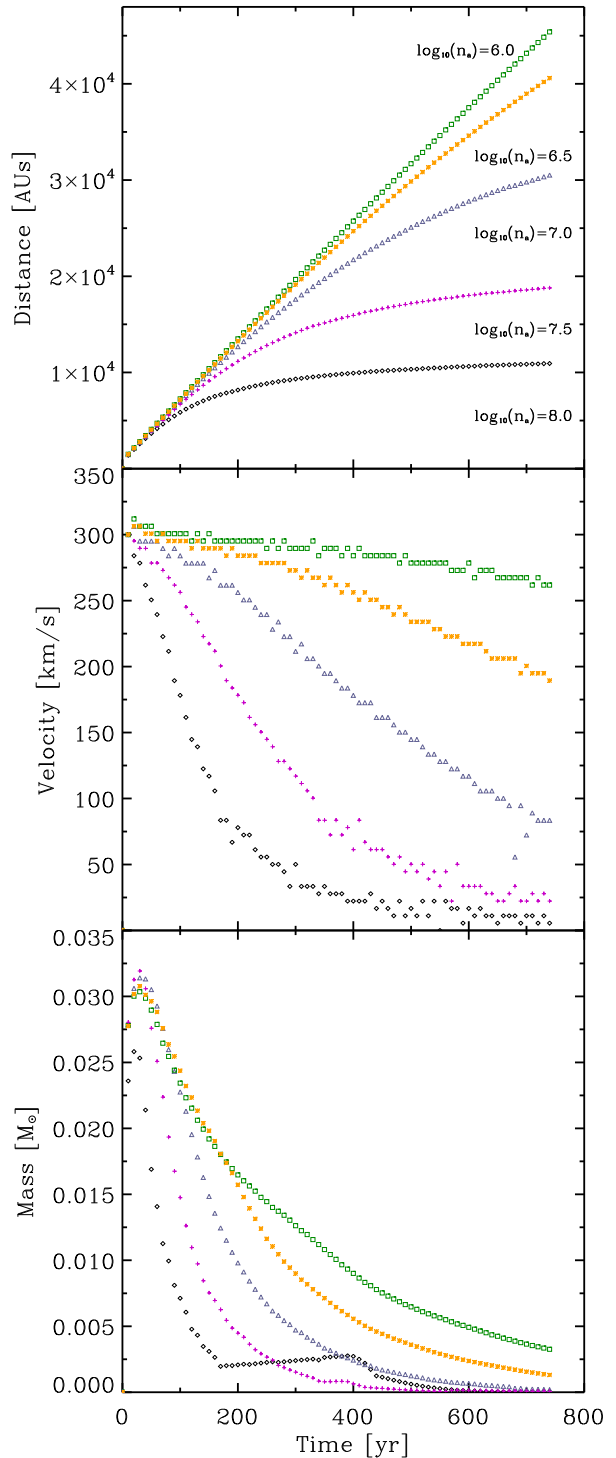


FIG. 2.— The top, middle and bottom panels shows the position, velocity and mass as function of time by the numerical model with initial velocities of 300 km s^{-1} , respectively. In each of this panels we plot the results obtained for the models evolving with logarithmic interstellar medium densities of 6, 6.5, 7, 7.5 and 8 using green squares, yellow asterisks, blue triangles, magenta crosses and black diamonds symbols, respectively.

of the numerical simulations for a larger initial velocity, 300 km s^{-1} . The results for the distance, velocity and

mass are very similar to those found in the models with initial velocity of 300 km s^{-1} . However, the deceleration for the models with initial velocity of 500 km s^{-1} is larger than those for the models with $v_0=300 \text{ km s}^{-1}$, and lifetime of the faster clumps is smaller than those for the lower ones, as we predicted in our Eq. (22).

Using the dimensionless mass of the clump and velocity from our numerical simulation in the Eq. (13) we fitted the α value for all the numerical model. Figure (4) shows the logarithm of the mass of the clump as function of velocity (dimensionless), for all the models with initial velocity of 300 km s^{-1} , we use the same nomenclature for the symbols as in the Figure (2), and the solid lines are the fit for the models, M1V300, M2V300, M3V300, M4V300, M5V300 and M6V300.

The α values for all the models presented here are plotted in Figure (5). The plus and diamond symbols are the α values fitted for modes with $v_0=300$ and 500 km s^{-1} , respectively. In order to obtain the value for the constant λ (see Eq. (19)), we have fitted the α values as function of the contrast density β to our numerical simulation (solid line in this figure). The best fit gives $\lambda = 0.0615$. Notice that the α values are only function of contrast density and these values are not dependent of the initial velocity or other parameters of the cloud, as described by Eq. (19). λ is a constant that is independent of the physical properties of the interstellar medium or clump gas.

4. PREDICTION OF EVOLUTIONARY PHYSICAL PROPERTIES OF THE PLASMON

The solution for a constant mass plasmon can be found from Eq. (13) with $\alpha = 0$. The results are,

$$u = \left(1 - \frac{\tau}{3}\right)^3, \quad (27)$$

for the velocity, and

$$r = \frac{3}{4} \left[1 - \left(1 - \frac{\tau}{3}\right)^4\right] \quad (28)$$

for the position.

Therefore, in the approximation of DA the lifetime of a plasmon is $t_f = 3 \cdot t_0$ (see Eq. (27)). When the mass loss rate is taking into account the plasmon's motion is changed, and the Eq. (13) can be integrated numerically to obtain u and the dimensionless position $r = x/x_0$ with $x_0 = v_0 t_0$. It is important to recall that C98 included the centrifugal pressure, which can affect the plasmon shape. This effect was not included in DA neither by us.

Finally, we use our numerical simulations to probe our models and their limitations. Each simulation has physical units, so they have to be normalized with v_0, t_0 and x_0 . v_0 is obtained directly from the initial conditions, t_0 is obtained from a fit of the velocity data and x_0 comes from a similar fit of the position data.

Figure (6) shows the dimensionless velocity as function of dimensionless time. From this figure, one can see that the DA solution agrees with the numerical results of the model M4V300 only for $\tau \leq 0.2$ (crosses). However, the semi-analytical solution, solid line is in agreement with the numerical model up to $\tau = 0.6$. Notice, that after $\tau = 0.6$ the values of u , for the numerical simulation, tends to a constant. There are numerical uncertainties

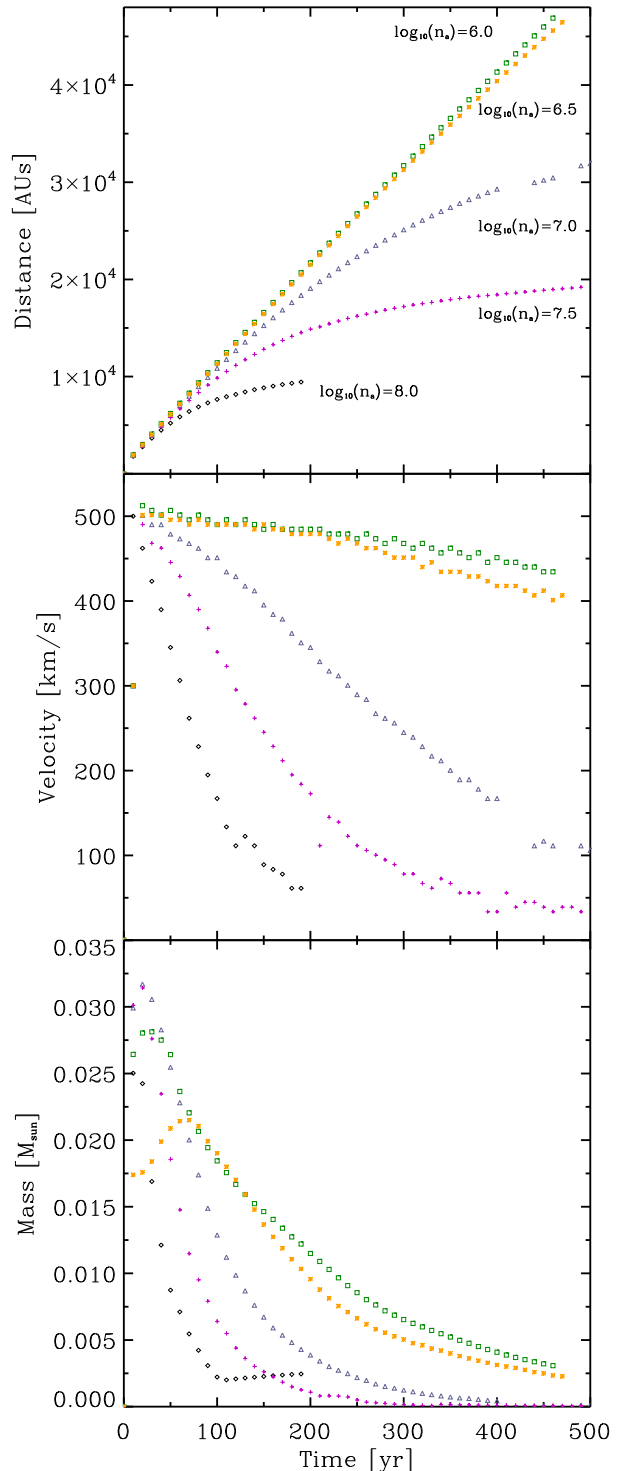


FIG. 3.— The same as Figure 2 but for models with initial velocity of 500 km s^{-1} .

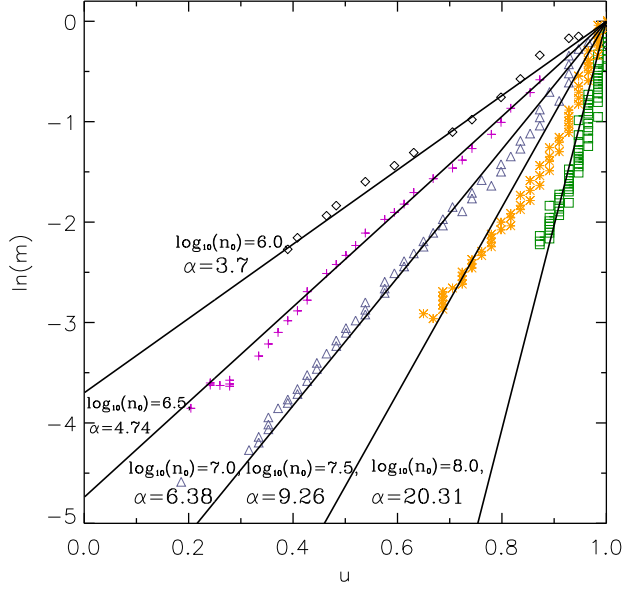


FIG. 4.— Mass of the clump as function of the clump’s velocity (dimensionless). The nomenclature of the symbols is the same as in the Figure (2) and in solid lines we plot the fit for each of the models with initial velocities of 300 km s^{-1} .

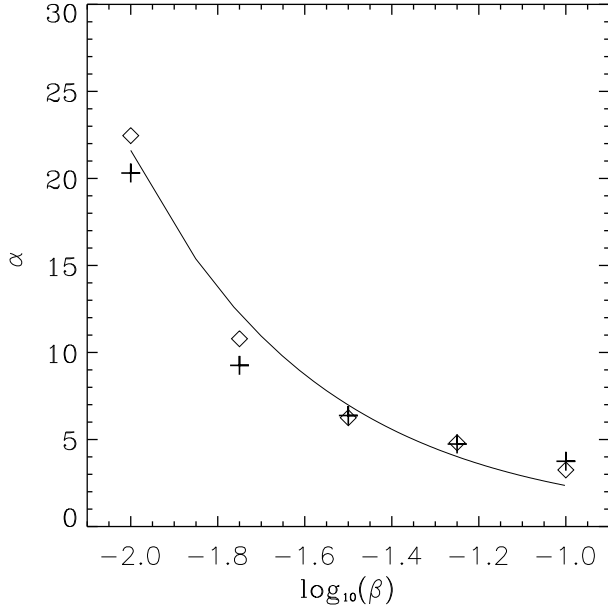


FIG. 5.— The constant α as function of contrast density (β). The plus and diamond symbols are the α values for models with $v_0=300$ and 500 km s^{-1} , respectively and the solid line is the best fit of λ (see Eq. 19), $\lambda=0.0615$.

that lead to overestimate the velocity, since, as the plasmon loses mass, it is difficult to determine its position and therefore its velocity.

Figure (7) shows the dimensionless position as function of dimensionless time. The DA solution, semi-analytic solution and numerical data are represented in this figure. The DA solution is similar to the numerical data for $\tau \leq 0.4$, while for the semi-analytical solution the agreement extends up to $\tau \simeq 0.6$. In the case of semi-

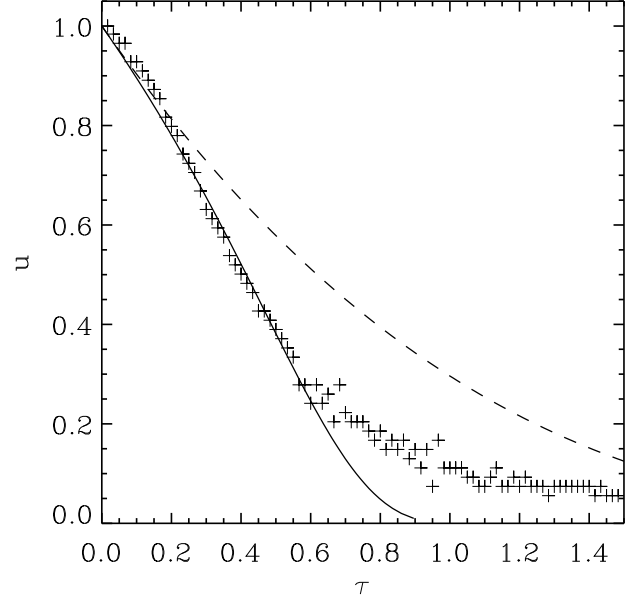


FIG. 6.— Dimensionless velocity, u , vs dimensionless time, τ , for the model with $\log \beta = -1.25$. Solid line represents the solution to Eq. 13, dashed line is the De Young and Axford prediction in Eq. 27 and crosses are the numerical simulation data normalized with $v_0 = 300 \text{ km s}^{-1}$ and $t_0 = 600 \text{ yr}$

analytical solution this time is as long as $\tau = 0.8$, similar stop distance while the DA model predicts a larger distance

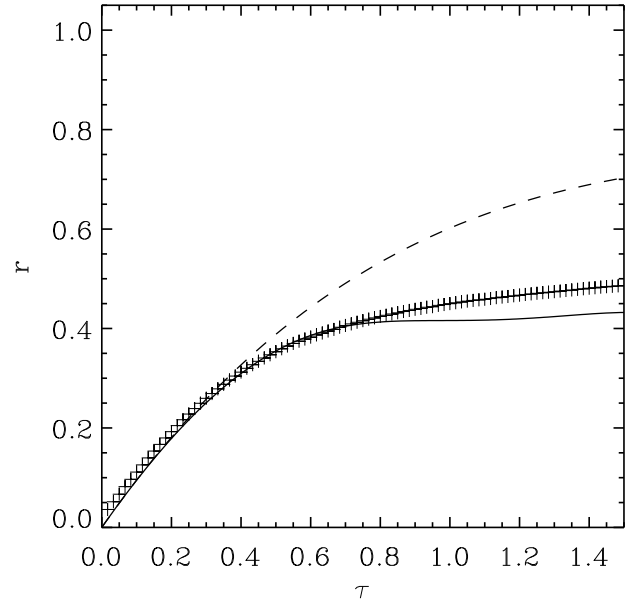


FIG. 7.— Dimensionless position r vs dimensionless time τ for the model with $\log \beta = -1.25$. Solid line represents the solution to Eq. (13), dashed line is the De Young and Axford prediction in Eq. (28) and crosses are the numerical simulation data normalized with $x_0 = 38000 \text{ AU}$ and $t_0 = 600 \text{ yr}$

Finally, the analytic t_0 and $x_0 = v_0 t_0$ obtained from Eq. (12) and the numerical t_0 and x_0 , for all the models presented in Table (2) and Table (3) for initial velocities

300 km s⁻¹ and 500 km s⁻¹, respectively.

TABLE 2

ANALYTIC AND NUMERICAL SCALE LENGTH x_0 AND TIME t_0 FOR MODELS WITH $v_0 = 300$ KM S⁻¹

$\log\left(\frac{n_a}{[\text{cm}^{-3}]}\right)$	Analytical		Numerical	
	x_0 [AU]	t_0 [yr]	x_0 [AU]	t_0 [yr]
6	1.14×10^6	18369	1.2×10^6	18400
6.5	363868	5868	200000	3000
7.	117000	1900	90000	1400
7.5	38231	616	38000	600
8	12762	205	18000	250

From the analytical solution, we can see that the final position (the scale length) are only function of the contrast density and it is not related with the velocity at which the clump was thrown, see Table (2) and Table (3). However, the lifetime of the plasmon or clump is depends on the initial velocity and the density contrast. The plasmon that were faster initially suffer a higher deceleration.

TABLE 3

ANALYTIC AND NUMERICAL SCALE LENGTH x_0 AND TIME t_0 FOR MODELS WITH $v_0 = 500$ KM S⁻¹

$\log\left(\frac{n_a}{[\text{cm}^{-3}]}\right)$	Analytical		Numerical	
	x_0 [AU]	t_0 [yr]	x_0 [AU]	t_0 [yr]
6	1.14×10^6	11022	1.1×10^6	10000
6.5	363868	3500	300000	2700
7.	117000	1134	90000	850
7.5	38231	370	40000	400
8	12762	123	19000	165

5. CONCLUSIONS

We have used the plasmon solution obtained by DA and the solution presented in C98 to propose an analytical solution of the plasmon's deceleration when mass is considered.

This leads to interpret mass as a function of the plasmon velocity related by a constant α . This α can be interpreted as a friction coefficient. We calculate its dependence on the density contrast between the plasmon and the surrounding environment.

Several numerical simulations were performed trying to compare the validity of our analytic model. An estimation of $\lambda = 0.0615$ was found.

The lifetime obtained from the simple plasmon model is greater than the expected by our losing mass considerations. The deceleration obtained by this method is more likely to be responsible for the age discrepancy in astronomical flows as the Orion fingers. Also, it is important to notice that a plasmon with greater ejection speed has a shorter lifetime, which can be observed on simulations.

The final length of a plasmon is not related to its shape and depends on the initial conditions of the plasmon.

We acknowledge support from PAPIIT-UNAM grants IN-109518 and IG-100218. P.R.R.-O. acknowledges scholarship from CONACyT-México and financial support from COZCyT. We thank an anonymous referee for helpful comments and corrections.

APPENDIX

SPEED OF SOUND

Consider a supersonic flow with velocity v_2 and density ρ_2 interacting with a medium at rest with density ρ_1 . The interaction produces two shocks S_1 and S_2 (see Figure (8)). Between the shocks there is a growing region that has a uniform velocity v_c and uniform pressure P . S_1 , the forward shock, moves with velocity v_{S1} and runs into the medium at rest, accelerating it to the velocity v_c , while S_2 , the reverse shock, moves with velocity v_{S2} into the impinging flow decelerating it to the same velocity v_c . The region has two parts: one has density ρ'_2 and temperature T'_2 and is filled by shocked flow 2, while the other part is filled by shocked medium 1 and has density ρ'_1 and temperature T'_1 . Note that the pressure of both regions is however the same. These two regions are separated by a contact discontinuity C . We further assume that the shocks are strong and parallel. On a frame of reference moving with shock S_2 , we can write,

$$\rho'_2 = \frac{\gamma + 1}{\gamma - 1} \rho_2, \quad (\text{A1})$$

$$v'_2 = \frac{\gamma - 1}{\gamma + 1} (v_2 - v_{S2}) = v_c - v_{S2}, \quad (\text{A2})$$

and

$$P = \frac{2}{\gamma + 1} \rho_2 (v_2 - v_{S2})^2, \quad (\text{A3})$$

where v'_2 is the post- S_2 shock flow velocity in this frame of reference and γ is the ratio of specific heats. Now, in a frame of reference that moves with shock S_1 , the jump conditions across the shock gives,

$$\rho'_1 = \frac{\gamma + 1}{\gamma - 1} \rho_1, \quad (\text{A4})$$

$$v'_1 = \frac{\gamma - 1}{\gamma + 1} (-v_{S1}) = v_c - v_{S1}, \quad (\text{A5})$$

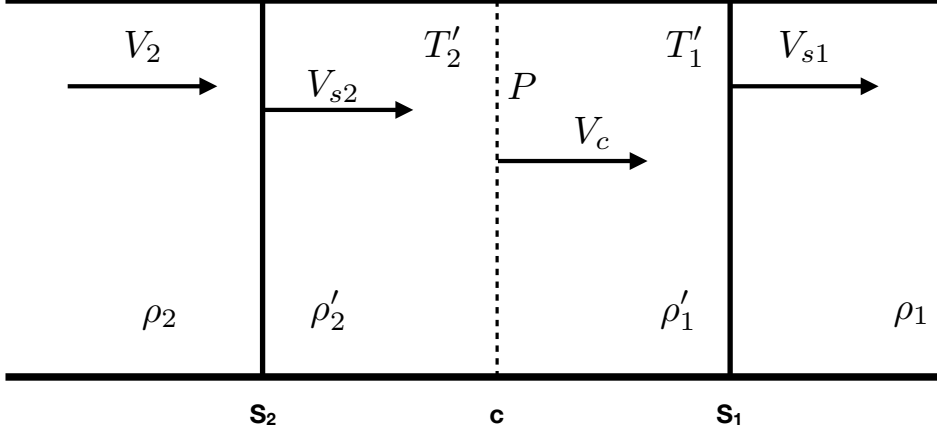


FIG. 8.— Scheme of the flow configuration produced by the interaction of a highly supersonic flow 2 with a gas at rest 1.

and

$$P = \frac{2}{\gamma + 1} \rho_1 (-v_{S1})^2, \quad (\text{A6})$$

where v'_1 is the post- S_1 shock velocity in this frame of reference.

From (A3) and (A6) we find

$$v_2 - v_{S2} = \beta v_{S1}, \quad (\text{A7})$$

where $\beta = (\rho_1/\rho_2)^{\frac{1}{2}}$.

Combining (A7) with (A2), (A5) and (A6) we find

$$v_c = \frac{v_2}{1 + \beta} \quad (\text{A8})$$

$$v_{S1} = \frac{\gamma + 1}{2(1 + \beta)} v_2 \quad (\text{A9})$$

$$v_{S2} = \frac{2 + \beta(1 - \gamma)}{2(1 + \beta)} v_2 \quad (\text{A10})$$

$$P = \frac{\gamma + 1}{2(1 + \beta)^2} \rho_1 v_2^2 \quad (\text{A11})$$

Finally, the isothermal sound speed behind shock S_2 is,

$$c_2 = \sqrt{\frac{P}{\rho'_2}} \quad (\text{A12})$$

$$c_2 = \left(\frac{\gamma - 1}{2}\right)^{1/2} \left(\frac{\beta}{1 + \beta}\right) v_2 \quad (\text{A13})$$

where we have used (A1) and the definition of β .

We can use Eq. (A12) to estimate the sound speed of the gas that was left behind by the reverse shock (shock S_2); that is the sound speed inside the plasmon. For this, we identify the impinging flow in the model presented in this Appendix with the original clump. So, if v_0 and ρ_{cl} are the launch velocity and density of the clump respectively, then, we take, $v_2 = v_0$, $\rho_2 = \rho_{cl}$ and ρ_1 equal to the density of the ambient medium through which the plasmon is moving ρ_a . Then, c_2 will be the sound speed inside the plasmon c , while v_c (from equation(A8)) will be the initial velocity of the plasmon v_0 . Substituting in Eq. (A13) we find,

$$c = v_0 \left(\frac{\gamma - 1}{2} \right)^{1/2} \beta. \quad (\text{A14})$$

REFERENCES

- Bally, J. and Cunningham, N. J. and Moeckel, N. and Burton, M. G. and Smith, N. and Frank, A. and Nordlund, A., 2011, *ApJ*, 113, 727
- Bally, J., 2016, *ARA&A*, 491, 54
- Cantó, J., Raga, A. 1991, *ApJ*, 372, 646.
- Cantó, J. and Espresate, J. and Raga, A. C. and D'Alessio, P., 1998, *MNRAS*, 1041, 296
- A. Castellanos-Ramírez, A. Rodríguez-González, P. R. Rivera-Ortiz, A. C. Raga, R. Navarro-González & A. Esquivel, 2018, *RMxAA*, 54, 409
- Daly, R. A., 1994, *ApJ*, 38, 426
- Daly, R. A., 1995, *ApJ*, 580, 454
- De Young, D. S. and Axford, W. I., 1967, *Nat*, 129-131, 216
- Esquivel A., Raga A. C., Cantó J., Rodríguez González, A., López-Cámara D., Velázquez P. F., De Colle F., 2010, *ApJ*, 725, 1466
- Henney, W. J. and Arthur, S. J. and de Colle, F. and Mellema, G., 2009, *MNRAS*, 157, 398
- Kahn, F.D., 1980, *Astron&Astrophys*, 83, 303
- Kosiński, R. and Hanasz, M., 2007, *MNRAS*, 861, 376
- Raga, A., Cabrit, S., Cantó, J. 1995, *MNRAS*, 273, 422.
- Raga, A. C. and Cantó, J. and Curiel, S. and Taylor, S., 1998, *MNRAS*, 738, 295
- Raga, A. C. and Reipurth, B., 2004, *RMxAA*, 15, 40
- Taylor, D. and Dyson, J. E. and Axon, D. J., 1992, *MNRAS*, 351, 255
- Toro, E. F., Spruce, M., & Speares, W. 1994, *Shock Waves*, 4, 25
- Ubachukwu, A. A. and Okoye, S. E. and Onuora, L. I., 1991, *ApJ*, 56, 383
- Veilleux, S. and Tully, R. B. and Bland-Hawthorn, J., 1993, *AJ*, 1318, 105
- Yalinewich, A. and Sari, R., 2016, *ApJ*, 177, 826
- Zapata, L. A. and Schmid-Burgk, J. and Ho, P. T. P. and Rodríguez, L. F. and Menten, K. M., 2009, *ApJ letters*, L45, 704